LEED and PIRS structure analysis of physisorbed molecules on insulators: Monolayer C_2D_2/KCl(100)

Jochen Vogt* and Helmut Weiss
Chemisches Institut der Universität Magdeburg, Universitätsplatz 2, D-39106 Magdeburg, Germany
(Received 11 January 2008; revised manuscript received 14 February 2008; published 14 March 2008)

The structure of the monolayer C_2D_2 adsorbed on a KCl(100) single crystal surface has been investigated by means of polarization infrared spectroscopy (PIRS) in transmission geometry at oblique incidence and low-energy electron diffraction (LEED). Infrared spectra in the region of the ν_3 asymmetric stretch vibration show at 75 K a singlet absorption at 2395.6 cm^{-1}. From the ratio of the integrated absorptions in *s*- and *p*-polarized spectra, a parallel orientation of the molecules with respect to the surface is deduced. The observed LEED diffraction patterns are consistent with a $(\sqrt{2}\times\sqrt{2})R45°$ lattice with two glide planes, in agreement with the parallel orientation of the molecules. LEED beam intensities of five inequivalent beams were recorded as a function of electron energy and the resulting $I(V)$ curves were analyzed using the tensor LEED approach. According to the $I(V)$ analysis and the analysis of the PIRS spectra, an adsorption geometry with two energetically equivalent but translationally inequivalent molecules in the surface unit cell is deduced with adsorption sites 3.14 Å above the K^+ cations. While IR spectroscopy supports a herringbone structure with the molecular axis of nearest neighbors intersecting at 90°, the LEED analysis is consistent with an intersection of 62°. These deviating results for the azimuthal orientations of the molecules on the KCl(100) surface are discussed within the concept of "split positions" [Over *et al.*, Phys. Rev. B **52**, 16812 (1995)] and the consideration of the in-plane libron dynamics of adsorbed molecules.

DOI: 10.1103/PhysRevB.77.125415 PACS number(s): 61.05.jh, 68.43.Fg, 68.43.Pq, 63.22.Np

I. INTRODUCTION

During the past decades, there has been a significant interest in studying the adsorption of small molecules on the surfaces of ionic materials. The reasons are manifold. One aspect is the only weak molecule-substrate interaction in these systems, which is governed predominantly by van der Waals forces. The latter are not supposed to affect the internal structure of the molecules. Ordered intermolecular structures, which are characterized by the positions and orientations of molecules in the adsorbate layer, arise as an effect of self-organization in an interplay between molecule-substrate and molecule-molecule interactions, leading in some cases to two-dimensional (2D) phases of high order. Therefore, these systems are sometimes characterized as *two-dimensional molecular crystals*. However, in most cases, the absolute positions and orientations of the molecules are not known.

By far, the most successful experimental technique for surface structure determinations is low-energy electron diffraction (LEED), more precisely, the quantitative analysis of diffraction peak intensities as a function of electron energy [$I(V)$ analysis].[1,2] A large number of surface structures of bare and adsorbate-covered metals and semiconductors has been investigated by means of this technique. Less work, however, has been done so far on the surface structures of clean and adsorbate-covered insulators. This is, to some extent, due to the difficulties arising when LEED experiments are performed on insulating surfaces, namely, the problems of surface charging and defect generation including the distortion or electron-stimulated desorption of molecular adsorbates. It has been shown that the use of a microchannel plate LEED (MCPLEED) optics for image amplification in combination with primary electron currents in the nanoampere range is a way to overcome these difficulties. In recent years, LEED structure analysis was thus extended also to wide band gap insulators.[3–6] $I(V)$ analyses from weakly bound molecules on insulating single crystals, however, are still rarely reported. We are only aware of studies on H_2O/MgO(100), C_2D_2/MgO(100), and CO_2/NaCl(100).[7–9]

Another valuable experimental technique, ideally suited for adsorption experiments on the surfaces of insulators and complementary to LEED, is polarization infrared spectroscopy (PIRS).[10,11] PIRS is sensitive to the orientation of induced vibrational dipole moments of molecules and, thus, to their orientation on the surface. Much of our knowledge on the adsorption of small molecules on the surfaces of insulators is due to this technique, which, if the lattice symmetry of an adsorbate is known by means of a diffraction technique such as LEED or helium atom scattering (HAS), can be combined with spectra simulations for structure determination.[12–21]

The concept which we pursue in this paper is a complete experimental determination of the adsorption geometry of C_2D_2 on KCl(100). Some experimental and theoretical work have been done on the related system C_2H_2/KCl(100).[21–23] The first layer of acetylene molecules forms a highly ordered $(\sqrt{2}\times\sqrt{2})R45°$ herringbone structure at 75 K, with two inequivalent molecules related by double glide-plane symmetry. This symmetry implies strictly parallel orientations of the molecules with respect to the surface plane and, moreover, an adsorption site either above K^+ or above Cl^-. A structure model which was based on these results is given in Fig. 1. However, the adsorption site, the distance of the molecules to the surface, and the azimuthal angles between two molecules in the adlayer unit cell are only predicted on the basis of potential calculations combining Lennard-Jones pair potentials and distributed multipoles.[22,23] The direct comparison of experimental results and theoretical predictions could show

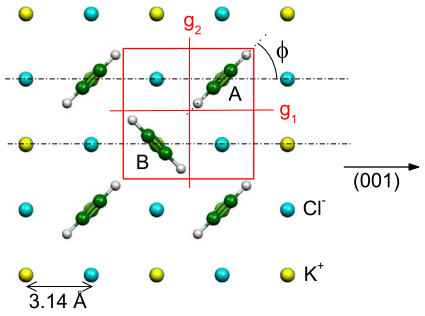

FIG. 1. (Color online) Structure model of the first layer acetylene on KCl(100) deduced from HAS (Refs. 22 and 23), PIRS, and LEED (Ref. 21) experiments (top view). The $(\sqrt{2}\times\sqrt{2})R45°$ unit cell (indicated as a box) contains two inequivalent molecules A and B. Their orientation is related by two glide planes g_1 and g_2. This leaves only three structure parameters, the adsorption site above K^+ or Cl^-, the azimuthal orientation ϕ of molecule A measured against the (001) direction, and its vertical distance x to the surface.

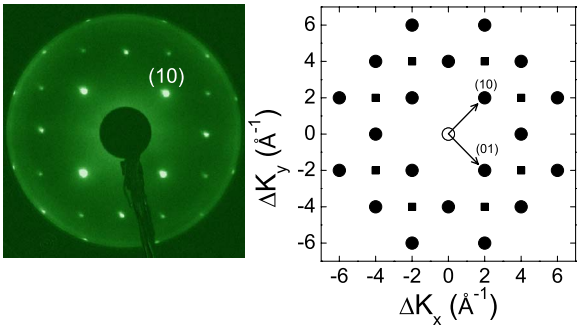

FIG. 2. (Color online) Left: LEED diffraction pattern of the monolayer C_2D_2/KCl(100), recorded at 75 K sample temperature and an electron energy of 130 eV. Right: Sketch of the reciprocal space indicating all observed beams of the $(\sqrt{2}\times\sqrt{2})R45°$ lattice, for which LEED $I(V)$ data have been recorded. Circles mark substrate spots and squares mark the additional superstructure spots observed at normal incidence.

how close experiment and theory can come in these systems.

This paper is organized as follows: In Sec. II, the experimental setup is summarized and the LEED and PIRS experiments are reported. In Sec. III, the LEED and PIRS spectra are analyzed and subsequently discussed in Sec. IV. Finally, the main results are summarized in Sec. V.

II. EXPERIMENT

A. Experimental setup

The setup of the experiments presented below is identical to the one described in Refs. 9 and 21 and we only provide the most essential features. It consists of an ultrahigh vacuum chamber, which is connected to a Fourier transform infrared spectrometer (Bruker IFS 120 HR) and an external detector box, and contains a double channel plate MCPLEED optics (Omicron).

A KCl single crystal (Korth Kristalle) with a front area of 20×20 mm^2 was cleaved in dry nitrogen atmosphere, and a slice of 3 mm thickness with two fresh (100) cleavage planes was mounted on a sample holder and transferred within 30 min into the UHV chamber. The sample holder is connected to the cold head of a closed-cycle helium refrigerator by means of a flexible copper braid. A minimum temperature of 20 K can be reached with this setup. The temperature is measured by means of a silicon diode (LakeShore) at the sample holder. Higher sample temperatures can be set with a stability of 0.1 K by means of an electrically insulated resistance heating. After bakeout, pressures of 3×10^{-10} mbar were reached. In order to avoid water contamination of the surface during cooling, the sample was initially held at temperatures above 300 K until the cold head reached a temperature below 150 K, thus acting as a cryopump and trapping residual gas molecules. Under measurement conditions, the base pressure was better than 1×10^{-10} mbar.

The sample crystal could be adjusted either with respect to the electron gun of the MCPLEED optics or with respect to the focus of the infrared beam. All IR experiments were performed in transmission geometry under oblique incidence conditions (angle of incidence $\beta=50°$ with respect to the surface normal) at a resolution of 0.2 cm^{-1}. The infrared signal was detected by means of a liquid nitrogen cooled InSb detector. For the recording of each spectrum, typically 32 interferogram scans were averaged and Fourier transformed using a Blackman–Harris apodization function. The LEED experiments were performed under normal incidence conditions (see below) at primary currents below 1 nA. Diffraction patterns were recorded using a slow-scan charge coupled device (CCD) camera with 4096 grayscales and 768 $\times512$ pixels lateral resolution. Each pattern was corrected for the dark current of the CCD chip as well as stray light from the chamber by subtracting a second image that was recorded with blocked electron beam. For the integration of beam intensities, a method similar to that given by Held *et al.*[24] was used.

Deuterated acetylene (Isotec, purity 2.0) was used without further purification and was admitted into the recipient by means of a leakage valve. Under these conditions, the front as well as the backside of the crystal were uniformly exposed to gas-phase acetylene. Mass spectra were recorded during the experiments in order to check the composition of the residual gas and to confirm the purity of the C_2D_2.

B. Low-energy electron diffraction experiments

The monolayer C_2D_2 on KCl(100) was prepared by exposing the bare KCl(100) surface at a temperature of 75 K to 5×10^{-9} mbar C_2D_2. Diffraction patterns, recorded continuously at an electron energy of 130 eV, indicated a steep increase of the (10) beam intensity and a drop of the (11) spot intensity during exposure, until after 10 min a state of saturation was reached. Moreover, already after 2 min of exposure, additional diffraction peaks at half-order positions $\left(\pm\frac{1}{2}\pm\frac{3}{2}\right)$ were clearly observed. In Fig. 2, a diffraction pattern with the observed superstructure is depicted. It was recorded after C_2D_2 dosage for 10 min. Consistent with previous HAS results[22] on C_2H_2/KCl(100), the first layer C_2D_2 on KCl(100) has $(\sqrt{2}\times\sqrt{2})R45°$ symmetry. Superstructure peaks at positions $\left(\pm\frac{1}{2}\pm\frac{1}{2}\right)$ and $\left(\pm\frac{3}{2}\pm\frac{3}{2}\right)$ are not observed

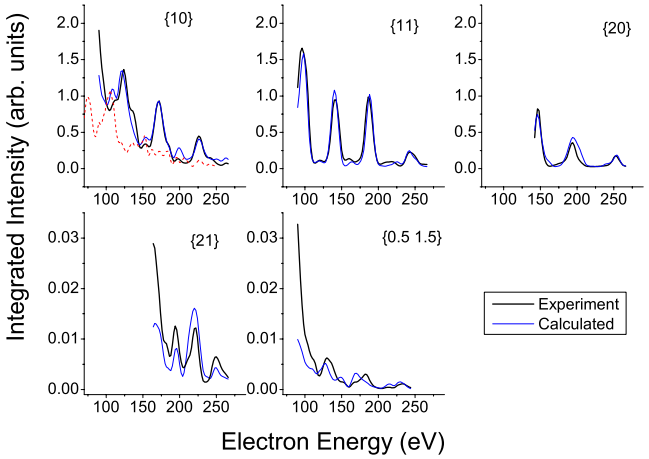

FIG. 3. (Color online) LEED $I(V)$ curves (bold lines) of the saturated 2D phase C_2D_2 adsorbed on the KCl(100) single crystal surface measured at 20 K. Also shown (thin lines) are the calculated $I(V)$ curves of the best-fit structure, corresponding to an overall Pendry R factor of 0.24. The dashed line in the diagram for the (10) beam order is a $I(V)$ curve of the bare KCl(100) surface.

over a wide energy range at normal incidence conditions. At an electron energy of 130 eV, however, small misalignments of the sample lead to the appearance of these forbidden spots, which is the ultimate proof of the presence of two glide planes[25] parallel to the directions (001) and (010). From the shape and width of the superstructure spots, the adsorbate can be judged to be highly ordered. Also shown in Fig. 2 is a sketch of the two-dimensional reciprocal space, indicating all diffraction beams for which integrated intensities were determined as a function of primary electron energy. The $I(V)$ curves from the saturated monolayer were recorded after the valve was closed and the crystal was cooled down to 20 K for intensity reasons. A series of diffraction patterns was taken in steps of 2 eV in the energy range between 90 and 270 eV. The $I(V)$ curves of symmetry equivalent diffraction spots were averaged and are depicted as bold lines in Fig. 3. For the (10) beam, a $I(V)$ profile of the bare KCl(100) surface is also given in the upper left diagram in Fig. 3. A comparison of the $I(V)$ profiles of the bare and adsorbate-covered KCl(100) surface shows marked differences for this beam order, namely, the appearance of three maxima near 122, 172, and 226 eV.

C. Polarization infrared spectroscopy experiments

In the infrared experiments, the bare KCl(100) sample was exposed to 5×10^{-9} mbar C_2D_2 at 75 K and IR spectra were continuously recorded in s and p polarizations. A pair of PIRS spectra, recorded after 10 min of gas exposure, is shown in Fig. 4. The formation of an acetylene adlayer on both the front and backside of the crystal was indicated by a rapid growth of a sharp absorption at 2395.6 cm^{-1}, which can unambiguously be assigned to the ν_3 asymmetric stretch mode of the major component $^{12}C_2D_2$, ~43 cm^{-1} redshifted with respect to the gas-phase transition.[26] In the solid state, Bottger and Eggers[27] have observed this transition at

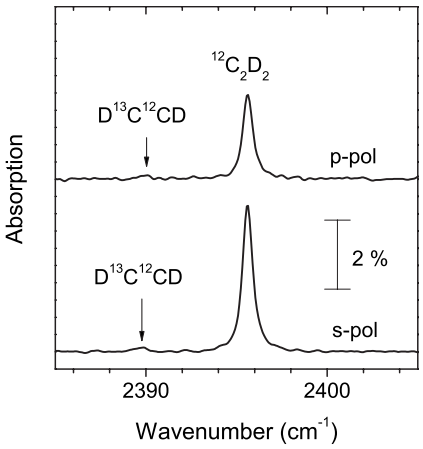

FIG. 4. Transmission infrared spectra of the monolayer C_2D_2/KCl(100) in the region of the ν_3 asymmetric stretch mode, recorded with s- and p-polarized light, respectively. The crystal temperature was 75 K.

2393.2 cm^{-1}. The observed spectroscopic data, such as transition wave number, integrated absorptions in s and p polarizations, and linewidth, are given in Table I. In the spectra shown in Fig. 4, a very weak absorption at 2389.7 cm^{-1} is also observed, which is attributed to a vibrational transition of the minor component $D^{13}C^{12}CD$. The latter has been observed[27] in crystalline C_2D_2 at 2387 cm^{-1}. Subsequently, the dosage was stopped and the crystal temperature was lowered to 20 K. The PIRS spectra recorded under these conditions revealed a further redshift of the observed IR absorption of about 1.7 cm^{-1} and a further narrowing of the linewidth, but no principal changes in the spectra.

III. RESULTS

A. Analysis of polarization infrared spectroscopy spectra

Polarization infrared spectroscopy from molecules adsorbed on insulator surfaces is sensitive to the inclination θ of induced vibrational dipole moments with respect to the surface plane.[10,11] This is due to the fact that the absorption strength is related to the square of the scalar product of the dipole moment and the electric field vector, which has different orientations for s- and p-polarized light, respectively.[10] The ratio of the integrated absorptions, A_s/A_p, can thus be used to determine the tilt angle of an induced vibrational dipole moment with respect to the surface plane,[16,18] while the presence of adsorbate domains with different orientations cancels the dependence on the azimuthal orientation ϕ. Based on a two-layer model (substrate+adsorbate), the

TABLE I. Characteristics of the observed IR spectra.

	s polarized	p polarized
Integrated absorption A (cm^{-1})	0.042	0.024
Transition wave number $\tilde{\nu}$ (cm^{-1})	2395.6	
Transition linewidth $\Delta\tilde{\nu}$ (cm^{-1})	0.66	

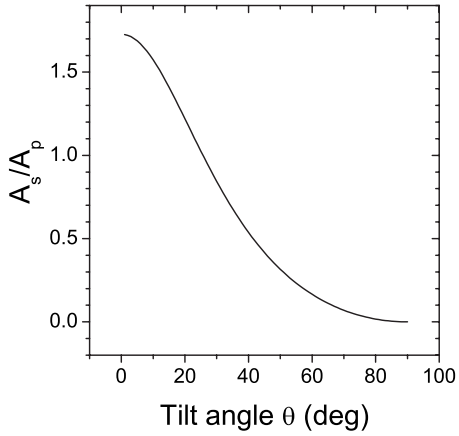

FIG. 5. Dependence of the ratio of integrated absorptions A_s/A_p on the molecular tilt angle θ, measured as determined from a two-layer model (angle of incidence $\beta=50°$, substrate index of refraction $n=1.47$ at 2400 cm^{-1}).

A_s/A_p ratio can be calculated by taking into account the electric fields at the frontside and at the backside of the KCl crystal (index of refraction $n=1.47$) by means of Fresnel's laws. For the angle of incidence $\beta=50°$ used in the experiments, the A_s/A_p ratio is plotted in Fig. 5 as a function of the tilt angle of the induced dipole moment. In the case of the ν_3 asymmetric stretch mode, the induced dipole moment is directed along the molecular axis. Hence, its tilt angle corresponds to the tilt angle of the molecule. From the values of the measured integrated absorptions A given in Table I, the experimental ratio A_s/A_p is 1.75, consistent with an exactly parallel orientation ($\theta=0°$) of the molecules with respect to the surface plane.

Further information on the adsorbate structure can be extracted from the IR experiments by means of spectra simulations. The measured spectra profiles contain only one single, sharp absorption in the ν_3 region. Yet in the case of a periodic structure with at least two energetically equivalent but translationally inequivalent molecules, a doublet of absorption bands is expected as a consequence of a coupling between induced electric dipoles, leading to collective excitations of in-phase and out-of-phase modes. Such Davydov or correlation-field splittings can be quite large, as found for the monolayer CO_2 $(2\times1)/NaCl(100)$,[16,17] where the monomer asymmetric stretch mode is split into two peaks, separated by more than 9 cm^{-1}. Dunn and Ewing[19,20] have shown that dipole-dipole coupling does also occur in the related system $C_2D_2/NaCl(100)$, where, however, a considerably smaller splitting of only 1.5 cm^{-1} was observed.[19,20] The correlation-field splitting depends strongly on the adsorbate structure and, moreover, on the infrared cross section σ of the vibrational mode. For a closed layer of C_2D_2, σ can be determined from the experimental spectra assuming a full monolayer capacity of 5.0×10^{14} molecules cm^{-2} on the frontside and on the backside of the crystal, the total measured integrated absorption (see Table I), and the conditions of oblique incidence of the IR beam. Based on this, $\sigma=4.2\times10^{-17}$ cm is estimated. With this information, it is straightforward to simulate PIRS spectra for various adsorbate geometries using the dynamic dipole-dipole coupling

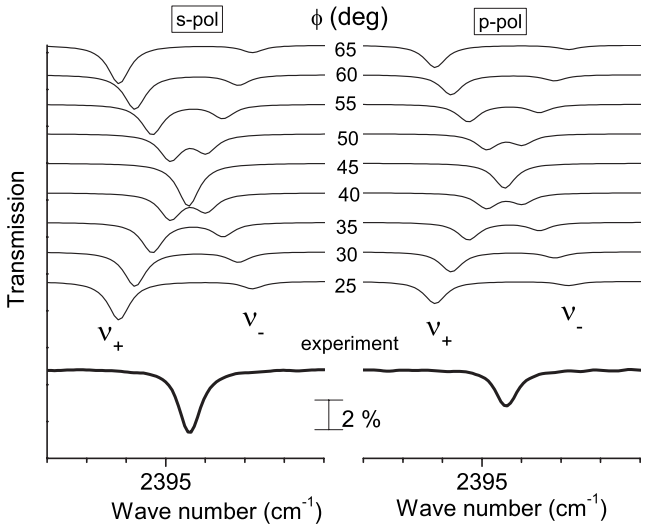

FIG. 6. Comparison between experimental PIRS spectra (bold line, bottom) and simulated spectra (thin lines) for the 2D $(\sqrt{2}\times\sqrt{2})R45°$ structure shown in Fig. 1 and various azimuthal orientations ϕ. The simulation of PIRS spectra was done according to the model outlined in Ref. 21 with the following simulation parameters: singleton frequency $\tilde{\nu}_0=2396.5$ cm^{-1}, linewidth $\Delta\tilde{\nu}=0.66$ cm^{-1}, and vibrational polarizability $\alpha_{vib}=0.059$ $Å^3$, corresponding to an integrated molecular absorption cross section of 4.2×10^{-17} cm.

approach.[28] Our implementation of this method has been outlined in detail in Ref. 21. The following constraints are given by the experiment: (1) the molecules must be oriented parallel to the KCl(100) surface, as evidenced by the measured A_s/A_p ratio and the observed two glide planes, which is impossible for inclined molecules; and (2) the center of mass of the molecules must be located either above K^+ or above Cl^- ions in the $(\sqrt{2}\times\sqrt{2})R45°$ unit cell, which constraints the distance of neigboring molecules to 4.44 Å, i.e., the cation-cation or the anion-anion nearest neighbor distance. In Fig. 6, pairs of simulated PIRS spectra are shown for various azimuthal orientations ϕ of the two molecules in the unit cell (see Fig. 1). In general, a doublet of IR absorptions ν_+ (in phase) and ν_- (out of phase) results. The splitting between these two modes depends on the azimuthal parameter and vanishes for $\phi=45°$. At this angle, adjacent molecules are oriented in an exactly T-shaped fashion and the two modes become decoupled and degenerate. As a result, from the spectra simulations in comparison with the measured IR spectra, an azimuthal orientation $\phi=45\pm2°$ of molecule A in Fig. 1 is thus deduced.

B. Tensor low-energy electron diffraction analysis

For the interpretation of the LEED $I(V)$ spectra presented in Sec. II, the Barbieri/Van Hove SATLEED package[29] was used with an extension described in Ref. 9. The Barbieri/Van Hove phase shift package[30] was used to calculate phase shifts of the elements K, Cl, C, and D using a periodically repeated slab geometry with the unit cell depicted in Fig. 1 and a precalculated muffin tin zero potential of bulk KCl.

The structural search proceeded in two steps. In the first step, the spherical wave amplitudes of a reference structure

TABLE II. Results of the structural analysis.

	TLEED (This work)	PIRS (This work)	MD (Ref. 22)
Distance x over K^+ cation (Å)	3.14 ± 0.07		3.35 (3.44)
Azimuthal orientation ϕ (deg)	59 ± 7	45 ± 3	45

are calculated as a function of primary electron energy, from which the "tensor" is constructed, which allows a rapid calculation of the reflected wave amplitudes and, thus, the $I(V)$ curves of any surface structure that moderately deviates from the reference geometry. On the basis of this first fully dynamical calculation, the second step consisted of the actual structural search, in which the $I(V)$ curves of the trial structures are compared with the experimental set of $I(V)$ curves. As a measure of agreement, the reliability factor proposed by Pendry, R_P, was used and systematically minimized by varying the real part of the inner potential V_0 and the structural parameters x and ϕ according to Powell's method of conjugate directions.[31] The search could, thus, be restricted to geometries with linear molecules, correct bond lengths, and all observed symmetry properties including the two glide planes. The structural search was performed for both possible adsorption sites above K^+ and above Cl^- and for different ranges of the vertical position x of the molecular center of mass, since it is known[1] that the validity of the tensor LEED approximation is limited to vertical displacements of only ~ 0.2 Å. For larger displacements, a new reference structure needs to be calculated.

Judging from the peak shapes of the experimental $I(V)$ profiles from the bare and the acetylene covered KCl(100) surface, the imaginary part of the inner potential was set to a fixed value of −3 eV. The calculated intensities of the diffraction peaks were compared to the experimental data after domain averaging of diffraction peak intensities. This accounts for the fact that for arbitrary structure parameters (x, ϕ), the substrate has a higher point symmetry (c_{4v}) than an adsorbate island, which can be oriented in four different ways on the surface with equal probability.

The result of the LEED structure analysis is summarized in Table II. The structure supported by the LEED experiments is characterized by an adsorption site of the molecules 3.14 ± 0.07 Å on top of the K^+ cation. The lateral orientation of the two molecules in the 2D unit cell is characterized by an azimuthal angle of $59 \pm 7°$ and, thus, a herringbone-like arrangement of the molecules. Error bars were calculated by means of Pendry's definition of error bars.[1] The optimum reliability factor is 0.24. The corresponding best-fit $I(V)$ curves are shown in Fig. 3 in comparison to the set of experimental data. In Fig. 7, the reliability factor is plotted as a function of the azimuthal angle ϕ and the distance x of the molecules to the surface. The minimum is indicated as a cross.

In a further calculation, the structural search was started from this optimum geometry, releasing glide-plane symmetry and all other constraints, except for those on the KCl lattice.

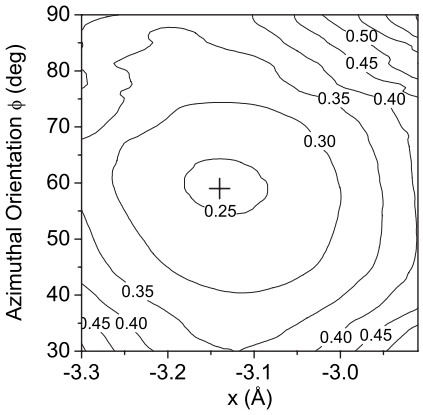

FIG. 7. Pendry R factor as a function of the structure parameters x (distance of the molecular center of mass to the surface) and ϕ (azimuthal orientation). The cross represents the optimum value at $R_p = 0.24$.

Hence, with the positions of all surface atoms being free to vary in the x, y, and z directions, the number of free parameters increased from $n=2$ to $n=24$. Under these conditions, the recalculated best-fit structure was characterized by only moderate overall shifts of the carbon atoms in the range of 0.17 Å (0.1 Å in vertical direction) and 0.22 Å of the hydrogen atoms. The reliability factor reached a considerably smaller value of 0.18. The improvement, however, is mainly caused by the increased number of fitting parameters, which gives a better compensation for statistical errors in the experimental $I(V)$ data. For this reason, the results of the $I(V)$ analysis without any structural constraints are not discussed further.

IV. DISCUSSION

Our discussion of the results starts with a combined inspection of the PIRS and LEED results for the geometry of the C_2D_2/KCl(100) $(\sqrt{2} \times \sqrt{2})R45°$ structure. The experimentally measured A_s/A_p ratio of the observed ν_3 absorption peak in the PIRS spectra as well as the observed double glide-plane symmetry in the LEED patterns strongly support a structure model with two molecules in the 2D unit cell, which have a parallel orientation with respect to the surface plane. Symmetry considerations leave only two independent structural parameters in this structure model, namely, the azimuthal orientation ϕ of the molecules and their distance x over the only two possible adsorption sites on top of Cl^- or on top of K^+. By means of tensor LEED, the adsorption site of the molecules is identified to be on top of the cation, in agreement with theoretical considerations based on pair potentials. The LEED experiment favors a center-of-mass distance of the molecules of 3.14 ± 0.07 Å to the surface, smaller than theoretical distances from the pair potentials applied in Ref. 22. The latter support larger distances to the surface, as can be seen in Table II: Depending on the applied potential model, theoretical values of 3.35 and 3.44 Å result. Although the differences between the experiment and the potential models are larger than the experimental error bars, the discrepancies are comparable to the typical uncertainties

in calculating molecule-surface distances even with more sophisticated quantum chemical methods. The above experimentally determined molecule-surface distance could, thus, serve as a benchmark for the refinement of theoretical models.

The second structural parameter is the azimuthal orientation of the molecules. In the PIRS spectra, an intense and sharp singlet absorption is visible, indicating degenerate in-phase and out-of-phase vibrational modes of the two molecules in the unit cell. Hence, according to the PIRS experiment, the molecules are oriented in an exactly T-shaped arrangement ($\phi=45\pm2°$). This result is in agreement with the theoretical results (see Table II). In contrast, the LEED structure analysis suggests this angle to be $\phi=59\pm7°$. One reason for this discrepancy could be the fact that the LEED diffraction peak intensities are by 1 order of magnitude more sensitive to vertical displacements of atoms than on lateral structural features,[1] making the LEED result for ϕ much less reliable than the PIRS result. However, there is an alternative and more profound explanation for the seeming contradiction between the two experiments if the influence of libronic motions of the molecules on the LEED intensities is taken into account. It is well known that, even at the lowest temperatures, the adsorbate lattice is not rigid. Instead, the molecules perform motions around their equilibrium positions, such as frustrated translations and rotations, i.e., external vibrational modes. Berg *et al.*[17] have analyzed the effect of libronic motions of adsorbed molecules on the IR spectra of internal modes in the system CO_2 $(2\times1)/NaCl(100)$. They point out that the structure parameters deduced from the IR spectrum of an internal mode reflect thermal averages. In this sense, the above value $\phi=45\pm2°$ deduced from the IR experiment is an average value ϕ_0.

In the case of the LEED experiments, Over *et al.*[32] demonstrated the effect of strong lateral movements of atoms and molecules and introduced the concept of split positions into LEED $I(V)$ analysis. According to this model, the effect of anisotropic lateral movements of atoms and molecules on LEED intensities is equivalent to a superposition of sets of split positions, in which the scatterers are displaced statically from their equilibrium positions. In the following, we adopt their model qualitatively. We investigate the effect of lateral frustrated rotations, as shown in Fig. 8, on the diffraction peak intensity I_g of a certain beam $\boldsymbol{g}$ before domain averaging is performed. According to Ref. 32, this intensity is given by the thermal average of beam amplitudes,

$$I_g = \langle A_g \rangle_T^2, \quad \langle A_g \rangle_T = \frac{1}{Z} \sum_{\boldsymbol{h}\in[\boldsymbol{g}]} \int A_{\boldsymbol{h}}(\Delta\phi) f(\Delta\phi, T) d\Delta\phi, \quad (1)$$

where $A_{\boldsymbol{h}}(\Delta\phi)$ is the amplitude of beam $\boldsymbol{h}$ if the molecules are rotated by an angle $\Delta\phi$ out of their equilibrium angle ϕ_0. Beam $\boldsymbol{h}$ is part of the set $[\boldsymbol{g}]$ of Z beams that are equivalent by the symmetry of the equilibrium structure shown in Fig. 1. Due to the frustrated rotations of the molecules, this symmetry is partially destroyed. To restore it in the thermal average, the respective beam amplitudes are averaged in Eq. (1). $f(\Delta\phi, T)$ is the probability density of finding a molecule

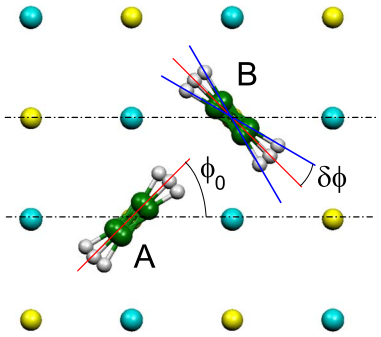

FIG. 8. (Color online) Lateral librations of the two C_2D_2 molecules A and B in the supercell. Shown is a superposition of three different local structures, corresponding to three different azimuthal orientations: equilibrium structure $\phi_0=45°$, and $\phi=\phi_0\pm\delta\phi$ with $\delta\phi=14°$ being the rms angle of frustrated rotations, deduced from the comparison of PIRS and LEED results and the adoption of the concept of "split positions" (Ref. 32).

displaced by an angle $\Delta\phi$. At low temperatures, this function can be assumed to be of Gaussian type,

$$f(\Delta\phi, T) = \frac{1}{\sqrt{2\pi}\delta\phi} \exp\left[-\frac{(\Delta\phi)^2}{2(\delta\phi)^2}\right]. \quad (2)$$

$\delta\phi$ is the temperature dependent rms value of the azimuthal deviation from the corresponding equilibrium value ϕ_0 at temperature T. For small $\Delta\phi$, $A_{\boldsymbol{h}}$ can be expanded up to second order. Insertion of Eq. (2) into Eq. (1) and evaluation of the integral, thus, yield

$$\langle A_g \rangle_T \approx \frac{1}{Z} \sum_{\boldsymbol{h}\in[\boldsymbol{g}]} \frac{1}{2}[A_{\boldsymbol{h}}(\phi_0+\delta\phi) + A_{\boldsymbol{h}}(\phi_0-\delta\phi)]. \quad (3)$$

For a given beam $\boldsymbol{h}$, the amplitudes $A_{\boldsymbol{h}}(\phi_0+\delta\phi)$ and $A_{\boldsymbol{y}}(\phi_0-\delta_\phi)$ are different in general. However, the analysis shows that for each beam $\boldsymbol{h}_1$ there is another beam $\boldsymbol{h}_2$ for which $A_{\boldsymbol{h}_1}(\phi_0+\delta\phi)=A_{\boldsymbol{h}_2}(\phi_0-\delta\phi)$. Therefore, after averaging the beam amplitudes coherently, the mean intensity of beam $\boldsymbol{g}$ is

$$I_g = \left| \frac{1}{Z} \sum_{\boldsymbol{h}\in[\boldsymbol{g}]} A_{\boldsymbol{h}}(\phi_0+\delta\phi) \right|^2 \quad (4)$$

and, thus, the same as that of a structure in which the molecules are statically displaced from the equilibrium angle by $\delta\phi$. Thus, within this model, deviating results for ϕ were expected and the difference of the best-fit values for the lateral orientation ϕ obtained from LEED $(59\pm7°)$ and PIRS $(45\pm2°)$ is consistent with a root mean square angle of in-plane libronic motions of the acetylene molecules of $\delta\phi=14\pm9°$ at 20 K.

In order to check if this value is conceivable, we estimate the 0 K rms amplitude for the in-plane libron mode on the basis of the theory of a harmonic librator. According to LeSar,[33] the mean square libronic amplitude of an acetylene molecule is given by

$$(\delta\phi)^2 = \frac{\hbar^2}{2IE}, \tag{5}$$

where I is the moment of inertia of the C_2D_2 molecule (32.8×10^{-47} kg m^2) and E is the libration excitation energy in harmonic approximation. In the case of undeuterated C_2H_2 molecules adsorbed on KCl(100), molecular dynamic calculations[22] predict in-plane libron modes to have an excitation energy of 16 meV, which is in excellent agreement with the value of 17 meV obtained from Hartree–Fock calculations of a $(KCl)_{25}(C_2H_2)_5$ cluster using basis sets of 6311-G(d,p) quality.[34] In the case of deuterated molecules, we obtain an excitation energy of 15 meV, which, by means of Eq. (5), is consistent with a 0 K rms libration angle of $\delta\phi=5°$. At a temperature of 20 K, thermal excitation is not expected to increase this value dramatically. Therefore, we conclude that the above value based on the model of split positions is too large, although just within the error bars. We think that the above considerations are useful in explaining the contradictory results of our LEED and PIRS experiments, but we also think that the structure model, which was based only on two structural parameters, is still too simple to yield reliable results for libration amplitudes. To become more accurate, a further study would be necessary, which would consider, e.g., in-plane and also out-of-plane external modes as additional structure parameters. This will be envisaged together with a systematic study of the effect of temperature on the LEED $I(V)$ curves. Moreover, it is known that the split-positions concept cannot discriminate between static disorder and dynamic disorder.[32] There are no indications for the presence of extensive static disorder in the acetylene layer, which could, for example, be deduced from an inhomogeneous broadening of the absorption line in Fig. 4. Nevertheless, a small amount of static disorder could also contribute to the discrepancy between the LEED and PIRS structure analysis.

V. CONCLUSIONS

The structure of the monolayer C_2D_2 adsorbed on KCl(100) was studied by means of PIRS and quantitative LEED at a temperature of 20 K. Based on the experimentally observed $(\sqrt{2}\times\sqrt{2})R45°$ lattice symmetry with two glide planes and a singlet absorption in the region of the ν_3 asymmetric stretch vibrational mode at 2395.6 cm^{-1}, a structure model containing two molecules per unit cell is proposed. The double glide-plane symmetry and also the observed ratio of infrared absorptions for s- and p-polarized light are consistent with a parallel orientation of the molecules with respect to the surface plane, leaving only two free structural parameters, i.e., the distance of the molecules either above the Cl^- anion or above the K^+ cations, and the azimuthal orientation of the molecules. The LEED analysis provides experimental evidence for the adsorption site: The center of mass of the C_2D_2 molecules is located 3.14 ± 0.07 Å above the cations. This distance is significantly smaller than predicted by theory.[22]

The analysis of the PIRS spectra based on photometric considerations in combination with spectra simulations supports an exactly T-shaped azimuthal orientation of adjacent molecules, while tensor LEED supports a lateral orientation in which the axes of neighboring molecules enclose an angle of $62\pm14°$. The reasons for this discrepancy may be that the LEED analysis is rather insensitive to the azimuthal orientation of the adsorbed molecules as well as the assumption of a strictly rigid adsorbate lattice in the LEED analysis. However, even at lowest temperatures, the adlayer molecules perform libration motions, which can be treated within the split-positions concept.[32] Consideration of lateral libration motions within this concept can explain the deviating results for the azimuthal orientations of the molecules from LEED and PIRS experiments qualitatively. The rms libration amplitude of $14\pm9°$ deduced from the experiments, however, is too large compared with theoretical estimations of the libration amplitudes.

ACKNOWLEDGMENT

Financial support by the Deutsche Forschungsgemeinschaft (DFG) is gratefully acknowledged.

*jochen.vogt@vst.uni-magdeburg.de

[1] M. A. Van Hove, W. Moritz, H. Over, P. J. Rous, A. Wander, A. Barbieri, N. Materer, U. Starke, G. A. Somorjai, Surf. Sci. Rep. **19**, 191 (1993).
[2] M. A. Van Hove, W. H. Weinberg, and C.-M. Chan, *Low-energy Electron Diffraction* (Springer, Berlin, 1986).
[3] D. Ferry, J. Suzanne, V. Panella, A. Barbieri, M. A. Van Hove, and J. P. Biberian, J. Vac. Sci. Technol. A **16**, 2261 (1998).
[4] J. Vogt and H. Weiss, Surf. Sci. **491**, 155 (2001).
[5] A. Gotte, A. G. Cabello-Cartagena, J. Vogt, and H. Weiss, Surf. Sci. **601**, 411 (2007).
[6] J. Vogt, Phys. Rev. B **75**, 125423 (2007).
[7] D. Ferry, P. N. M. Hoang, J. Suzanne, J. P. Biberian, and M. A. Van Hove, Phys. Rev. Lett. **78**, 4237 (1997).
[8] D. Ferry, S. Picaud, P. N. M. Hoang, C. Girardet, L. Giordano, B. Demirdjian, and J. Suzanne, Surf. Sci. **409**, 101 (1998).
[9] J. Vogt and H. Weiss, J. Chem. Phys. **119**, 1105 (2003).
[10] Y. J. Chabal, Surf. Sci. Rep. **8**, 211 (1988).
[11] V. P. Tolstoy, I. V. Chernyshova, and V. A. Skryshevsky, *Handbook of Infrared Spectroscopy of Ultrathin Films* (Wiley, New York, 2003).
[12] J. Heidberg, M. Suhren, and H. Weiss, J. Electron Spectrosc. Relat. Phenom. **64/65**, 227 (1993).
[13] J. Heidberg, E. Kampshoff, and M. Suhren, J. Chem. Phys. **95**, 9408 (1991).
[14] D. A. Boyd, F. M. Hess, and G. B. Hess, Surf. Sci. **519**, 125 (2002).
[15] J. Vogt and H. Weiss, Z. Phys. Chem. **218**, 973 (2004).
[16] J. Heidberg, E. Kampshoff, O. Schönekäs, H. Stein, and H. Weiss, Ber. Bunsenges. Phys. Chem. **94**, 112 (1990).

[17] O. Berg, R. Disselkamp, and G. E. Ewing, Surf. Sci. **277**, 8 (1992).
[18] J. Heidberg, M. Hustedt, E. Kampfshoff, and V. M. Rozenbaum, Surf. Sci. **427–428**, 431 (1999).
[19] S. K. Dunn and G. E. Ewing, J. Phys. Chem. **96**, 5284 (1992).
[20] S. K. Dunn and G. E. Ewing, J. Vac. Sci. Technol. A **11**, 2078 (1993).
[21] J. Vogt, Phys. Rev. B **73**, 085418 (2006).
[22] A. L. Glebov, V. Panella, J. P. Toennies, F. Traeger, H. Weiss, S. Picaud, P. N. M. Hoang, and C. Girardet, Phys. Rev. B **61**, 14028 (2000).
[23] J. P. Toennies, F. Traeger, H. Weiss, S. Picaud, and P. N. M. Hoang, Phys. Rev. B **65**, 165427 (2002).
[24] G. Held, S. Uremovic, C. Stellwag, and D. Menzel, Rev. Sci. Instrum. **67**, 378 (1996).
[25] B. W. Holland and D. P. Woodruff, Surf. Sci. **36**, 488 (1973).
[26] W. M. A. Smit, A. J. Van Straten, and T. Visser, J. Mol. Struct. **48**, 177 (1978).
[27] G. L. Bottger and D. F. Eggers, J. Chem. Phys. **40**, 2010 (1964).
[28] B. N. J. Persson and R. Ryberg, Phys. Rev. B **24**, 6954 (1981).
[29] M. A. Van Hove, Barbieri/Van Hove SATLEED package.
[30] M. A. Van Hove, Barbieri/Van Hove phase shift package.
[31] M. J. D. Powell, Comput. J. **7**, 155 (1964).
[32] H. Over, M. Gierer, H. Bludau, and G. Ertl, Phys. Rev. B **52**, 16812 (1995).
[33] R. LeSar, J. Chem. Phys. **86**, 1485 (1987).
[34] J. Vogt and H. Weiss (unpublished).